Structure and function of the yeast listerin (Ltn1) conserved N-terminal domain in binding to stalled 60S ribosomal subunits

Selom K. Doamekpor[a,1], Joong-Won Lee[b,1,2], Nathaniel L. Hepowit[b], Cheng Wu[c], Clement Charenton[a], Marilyn Leonard[b], Mario H. Bengtson[b,3], Kanagalaghatta R. Rajashankar[d,e], Matthew S. Sachs[c,4], Christopher D. Lima[a,f,4], and Claudio A. P. Joazeiro[b,g,h,4]

[a]Structural Biology Program, Sloan–Kettering Institute, New York, NY 10065; [b]Department of Cell and Molecular Biology, The Scripps Research Institute, La Jolla, CA 92037; [c]Department of Biology, Texas A&M University, College Station, TX 77843-3258; [d]Northeastern Collaborative Access Team, Advanced Photon Source, Argonne, IL 60439; [e]Department of Chemistry and Chemical Biology, Cornell University, Ithaca, NY 14853; [f]Howard Hughes Medical Institute, Sloan–Kettering Institute, New York, NY 10065; [g]Zentrum für Molekulare Biologie der Universität Heidelberg, Heidelberg D-69120, Germany; and [h]Deutsches Krebsforschungszentrum–Zentrum für Molekulare Biologie der Universität Heidelberg Alliance (ZMBH-DKFZ), Heidelberg D-69120, Germany

Edited by Tony Hunter, The Salk Institute for Biological Studies, La Jolla, CA, and approved May 25, 2016 (received for review April 15, 2016)

The Ltn1 E3 ligase (listerin in mammals) has emerged as a paradigm for understanding ribosome-associated ubiquitylation. Ltn1 binds to 60S ribosomal subunits to ubiquitylate nascent polypeptides that become stalled during synthesis; among Ltn1's substrates are aberrant products of mRNA lacking stop codons [nonstop translation products (NSPs)]. Here, we report the reconstitution of NSP ubiquitylation in *Neurospora crassa* cell extracts. Upon translation in vitro, ribosome-stalled NSPs were ubiquitylated in an Ltn1-dependent manner, while still ribosome-associated. Furthermore, we provide biochemical evidence that the conserved N-terminal domain (NTD) plays a significant role in the binding of Ltn1 to 60S ribosomal subunits and that NTD mutations causing defective 60S binding also lead to defective NSP ubiquitylation, without affecting Ltn1's intrinsic E3 ligase activity. Finally, we report the crystal structure of the Ltn1 NTD at 2.4-Å resolution. The structure, combined with additional mutational studies, provides insight to NTD's role in binding stalled 60S subunits. Our findings show that *Neurospora* extracts can be used as a tool to dissect mechanisms underlying ribosome-associated protein quality control and are consistent with a model in which Ltn1 uses 60S subunits as adapters, at least in part via its NTD, to target stalled NSPs for ubiquitylation.

Listerin | Ltn1 | RQC | ribosome | structure

The conservation of the Ltn1 E3 ligase among eukaryotic organisms suggests that it has an important function; accordingly, mutations of the Ltn1 mouse ortholog can cause embryonic lethality or neurodegeneration (1). Using *Saccharomyces cerevisiae* as a model to elucidate Ltn1's function, we uncovered a role for yeast Ltn1 (also known as Rkr1) in a pathway of protein quality control (PQC) that is associated with the 60S ribosomal subunit (2). This finding was important because, although it has long been known that PQC mechanisms are critical to maintain protein homeostasis and cellular fitness, only a few pathways mediating the surveillance of aberrant proteins in eukaryotes have been uncovered to date (3–6). In addition, because defective PQC is a hallmark of neurodegenerative diseases (3–6), the above findings suggested that the Ltn1 yeast model might be predictive of basic molecular mechanisms underlying the mouse neurodegenerative phenotype.

Ltn1 orthologs are ∼150- to 180-kDa proteins harboring an E3-catalytic RING domain at the C-terminal end, and an N-terminal domain (NTD) (2). These two conserved regions are separated by a long HEAT repeat domain of ∼85 kDa that is less conserved at the primary amino acid sequence level (2, 7). Our studies in yeast had uncovered Ltn1 as the critical E3 ligase targeting aberrant proteins encoded by mRNA lacking stop codons ("nonstop mRNA") for ubiquitylation and proteasomal degradation (2). Ribosomes translating nonstop mRNA proceed through the poly(A) tail, which encodes polyLys. Presumably due to electrostatic interactions with the ribosomal nascent chain exit tunnel, nascent polyLys causes translation elongation to halt (8–10), eventually leading to the recruitment of Ltn1, which is vastly substoichiometric with regard to translating ribosomes (2). This phenomenon is not specific to poly-Lys because fusing a homopolymeric tract of either Lys or Arg to a stop codon-containing reporter protein, as well as internal polybasic tracts in endogenous proteins, is able to halt translation and promote Ltn1-mediated degradation (11–13). Furthermore, it is now known that other mechanisms preventing translational elongation or termination (e.g., mRNA truncation) can also result in Ltn1-mediated ubiquitylation of nascent chains (e.g., refs. 13 and 14).

There is no evidence to suggest that Ltn1 itself can directly sense elongation-halted ribosomes; rather, it has been proposed that such ribosomes are instead primary substrates of ribosome-splitting

Significance

The listerin (Ltn1) E3 ubiquitin ligase ubiquitylates and promotes degradation of aberrant nascent chains that become stalled on ribosomal 60S subunits. Ltn1-dependent nascent chain ubiquitylation was reconstituted in vitro using extracts of genetically manipulated *Neurospora* strains. Such extracts, supplemented or not with recombinant factors (such as Ltn1 from *Saccharomyces cerevisiae*), represent a new system to study ribosome-associated protein quality control. Utilizing this system, we show that mutations in Ltn1's conserved N-terminal domain result in defective 60S binding and nascent chain ubiquitylation, without affecting Ltn1's intrinsic E3 activity. Furthermore, we have solved the crystal structure of Ltn1's N-terminal domain, which provides detailed information and insights into how Ltn1 interacts with stalled 60S subunits. Our observations shed light on how cells handle protein quality control substrates.

Author contributions: S.K.D., J.-W.L., N.L.H., C.W., M.H.B., M.S.S., C.D.L., and C.A.P.J. designed research; S.K.D., J.-W.L., N.L.H., and C.W. performed research; C.W., C.C., M.L., and M.S.S. contributed new reagents/analytic tools; S.K.D., J.-W.L., N.L.H., C.W., M.H.B., K.R.R., M.S.S., C.D.L., and C.A.P.J. analyzed data; and S.K.D., J.-W.L., M.S.S., C.D.L., and C.A.P.J. wrote the paper.

The authors declare no conflict of interest.

This article is a PNAS Direct Submission.

Data deposition: The atomic coordinates and structure factors have been deposited in the Research Collaboratory for Structural Bioinformatics Protein Data Bank, www.pdb.org [PDB ID codes 5FG0 (native Ltn1) and 5FG1 (selenomethionine-substituted Ltn1)].

[1]S.K.D. and J.-W.L. contributed equally to this work.

[2]Present address: Eutilex Co., Ltd., College of Medicine, The Catholic University of Korea, 222 Banpo-Daero, Seocho-gu, Seoul 06591, Korea.

[3]Present address: Department of Biochemistry and Tissue Biology, Institute of Biology, University of Campinas (UNICAMP), Campinas, SP 13083-970, Brazil.

[4]To whom correspondence may be addressed: Email: joazeiro@scripps.edu, msachs@bio.tamu.edu, or limac@mskcc.org.

This article contains supporting information online at www.pnas.org/lookup/suppl/doi:10.1073/pnas.1605951113/-/DCSupplemental.

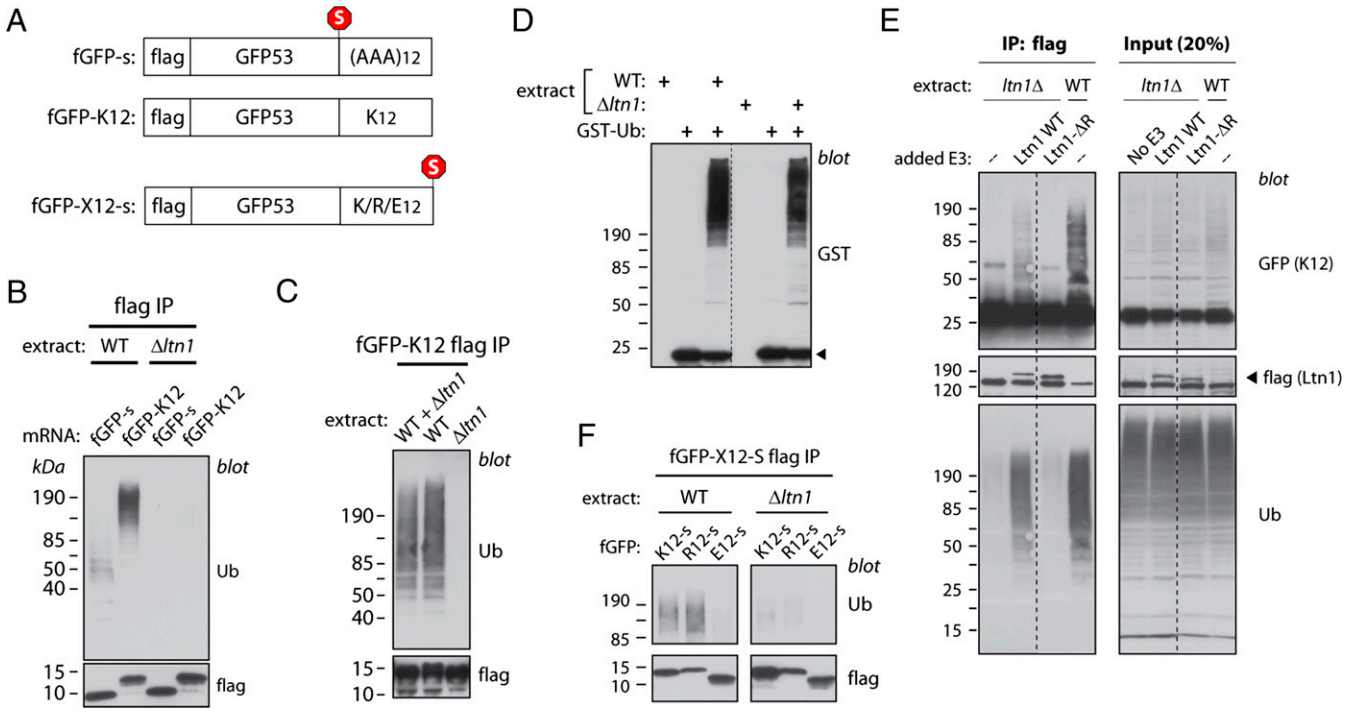

Fig. 1. Newly synthesized NSPs are ubiquitylated in *Neurospora* extracts in an Ltn1-dependent manner. (*A*) Diagram of templates used for in vitro translation, encoding flag-GFP53 (fGFP-s), the equivalent nonstop protein (fGFP-K12), equivalent proteins fused to homopolymeric tracts of 12 lysines (fGFP-K12-s), arginines (fGFP-R12-s), or glutamates (fGFP-E12-s); "s" indicates that the encoding mRNA harbor four in-frame stop codons. (*B*) Nonstop proteins synthesized in *Neurospora* extracts become ubiquitylated in an Ltn1-dependent manner. Three hundred nanograms of mRNA encoding fGFP-s or fGFP-K12 reporters were used to program translation reactions (30 μL) prepared from WT or Ltn1-deficient (Δ*ltn1*) strains for 30 min. Reaction products denatured with 1% SDS were diluted 10-fold and used for immunoprecipitation (IP) using anti-flag antibody. IPed proteins were used for immunoblots against ubiquitin (Ub) or flag. (*C*) The NSP ubiquitylation defect of Ltn1-deficient extracts is not due to the presence of *trans*-acting inhibitors. fGFP-K12 was synthesized in WT or Δ*ltn1* extracts, or in a 1:1 WT:Δ*ltn1* extract mixture. Reaction products were analyzed for ubiquitylation as in *B*. (*D*) Ltn1-deficient extracts are competent for de novo ubiquitylation. WT and Δ*ltn1* extracts were incubated with GST-tagged ubiquitin (GST-Ub; 10 μM) in the presence of 1 mM ATP for 10 min at 26 °C as indicated, and the ligation of GST-Ub to proteins in the extract (as revealed by the formation of a smear) was examined by anti-GST immunoblot. The arrowhead indicates free GST-Ub. Dashed lines indicate that lanes were removed from the original image. (*E*) Recombinant Ltn1 restored NSP ubiquitylation activity to Δ*ltn1* extracts. Recombinant, flag-tagged WT yeast Ltn1 or a mutant lacking the catalytic RING domain (Ltn1-ΔR) was added at 40 nM to Δ*ltn1* extract, as indicated, before translation using 300 ng of fGFP-K12-encoding mRNA (full-length GFP used for this experiment). Ubiquitylation of fGFP-K12 was measured as in *B*. Dashed lines indicate that lanes were removed from the original image. (*F*) Proteins encoded by stop codon-containing mRNA, but harboring polybasic tracts, are targeted by Ltn1. WT or Δ*ltn1* extracts were programmed with 300-ng templates encoding fGFP appended with a C-terminal tract of 12 Lys, Arg, or Glu, as represented in *A*. Reaction products were analyzed for ubiquitylation as in *B*.

rescue systems such as Dom34-Hbs1-Rli1 (13, 15–17). Dom34/Pelota and Hbs1 are homologous to the translation termination factors eRF1 and eRF3, respectively. The Hbs1 GTPase loads Dom34 onto translationally halted ribosomes in a stop codon-independent manner, followed by Hbs1 dissociation and Dom34-mediated recruitment of the Rli1/ABCE1 ATPase; Rli1, in turn, mediates splitting of the 60S and 40S subunits (15–17). However, unlike eRF1, Dom34 lacks nascent peptidyl-tRNA hydrolase activity. As a result, among the products of the Dom34-mediated reaction are 60S subunits that remain stalled with tRNA-conjugated nascent chains; it is such an abnormal complex that seems to be targeted by Ltn1 (13, 15–17). Consistent with these findings, Hbs1 was required upstream of Ltn1 for stalled chain ubiquitylation in the rabbit reticulocyte lysate (RRL) system (13), and Ltn1 is predominantly associated with 60S ribosomal subunits in steady state (2, 11, 12).

Ltn1 has been found to function as a subunit of the ribosome-associated protein quality control (RQC) complex (11, 12). In this complex containing stalled 60S subunits, the Rqc2/Tae2 subunit was initially shown to function in stabilizing Ltn1 binding (12). Ltn1's E3 activity and the Rqc1 subunit of the complex were both required for recruitment of the AAA ATPase Cdc48/p97/VCP and its cofactors Npl4 and Ufd1 (11, 12, 18). Finally, Cdc48 was proposed to extract the ubiquitylated nascent polypeptide from the stalled 60S subunit and deliver it to the proteasome (18). Thus, Ltn1-mediated ubiquitylation seems to play a role both in extracting stalled chains and in targeting them for elimination.

More recently, cryo-EM structures of Ltn1/listerin in complex with Rqc2/NEMF and stalled 60S subunits have been published (19–21). The structures suggest that Rqc2 recognizes the stalled 60S subunit by simultaneously binding to the tRNA moiety of the stalled peptidyl-tRNA and the 60S intersubunit surface. The Ltn1 NTD and C-terminal domain (CTD) both provide contacts within the RQC; the NTD binds both Rqc2 and the 60S in the vicinity of the sarcin-ricin loop (SRL) such that it would clash with the 40S subunit if that subunit were present whereas the RWD domain binds near the opening of the nascent chain exit tunnel (the RWD is a domain structurally related to ubiquitin-conjugating enzymes that is found in certain RING domain- or WD repeat-containing proteins, and in DEAD-like helicases). Ltn1's HEAT repeat-containing middle region serves as a linker between NTD and CTD bound to distal sites, providing an explanation for size conservation among Ltn1 orthologs. The cryo-EM structures remain incomplete, however, with components still missing and with several regions in which the resolution was insufficient to resolve amino acid side chains.

Although studies with *S. cerevisiae* have enabled elucidation of Ltn1's function and the pathways in which it is involved, it is critical to put the models derived from work using that system to test with alternative approaches, such as biochemical reconstitutions in which mechanisms can be examined. Along these lines, a robust RRL-based

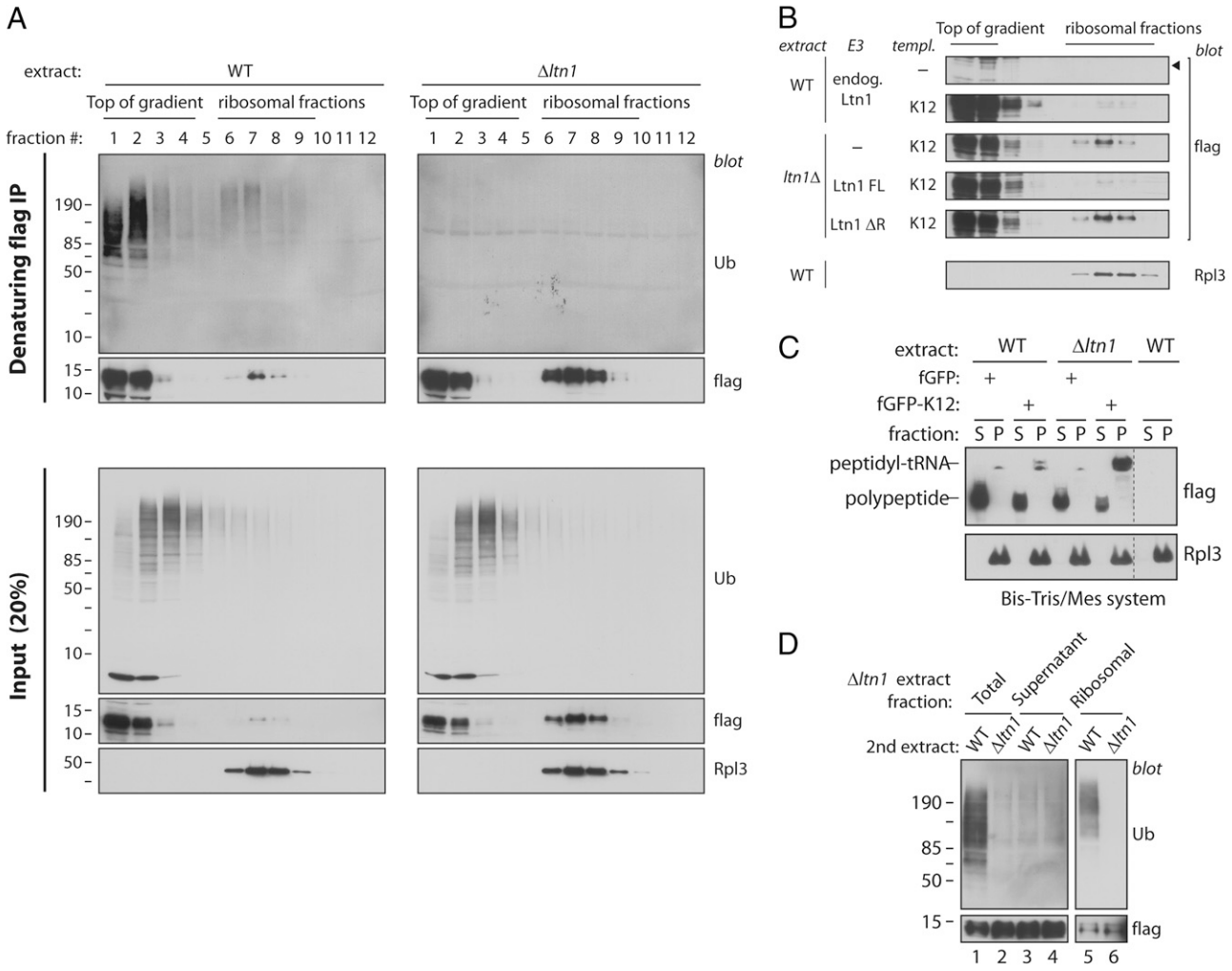

Fig. 2. Ltn1-mediated ubiquitylation of NSPs occurs on ribosomes. (*A*) Evidence for NSP ubiquitylation on ribosomes. Five hundred nanograms of fGFP-K12-encoding mRNA was translated for 30 min in 50 μL of WT or Δ*ltn1* extracts. Reaction products were separated by centrifugation in 15–40% (wt/vol) sucrose gradient; 20% of each fraction was analyzed by immunoblot against ubiquitin (Ub), flag, or the 60S ribosomal protein, Rpl3 ("Input"). The remaining material from each fraction was used for denaturing flag IPs (as in Fig. 1*B*) and analyzed by immunoblot against Ub or flag. (*B*) Five hundred nanograms of fGFP-K12–encoding mRNA was translated for 30 min in 50 μL of WT extract or in Δ*ltn1* extract supplemented or not with 40 nM recombinant yeast Ltn1 (WT or Ltn1-ΔR mutant, as indicated). Reaction products were separated by centrifugation in 15–40% (wt/vol) sucrose gradient. Fractions were analyzed by immunoblot against flag or Rpl3. (*C*) Evidence for tRNA-conjugated fGFP-K12 in ribosomal pellets. Two hundred nanograms of mRNA encoding fGFP-s or fGFP-K12 proteins were incubated with WT or Δ*ltn1* extracts (20 μL) for 30 min. Reaction products were separated by centrifugation on sucrose cushion; 40% of recovered supernatant ("S") and 100% of resuspended pellet ("P") were separated by electrophoresis in Bis-Tris gel containing Mes buffer, pH 6.8 (conditions under which peptidyl-tRNA is more stable) and analyzed by immunoblot against flag or Rpl3. Dashed lines indicate that lanes were removed from the original image. (*D*) Ribosome-stalled but not free NSPs are modified by Ltn1. Three hundred nanograms of fGFP-K12–encoding mRNA were translated in 30 μL of Δ*ltn1* extract for 30 min, followed by cycloheximide addition. To one set of reactions (lanes 1 and 2), fresh WT or Δ*ltn1* extract was added (1:1) and incubated for another 30 min before denaturing flag IP. In another set of reactions, products of the fGFP-K12 translation reaction in Δ*ltn1* extract were separated by centrifugation on sucrose cushion. Supernatant and the resuspended ribosome-containing pellet were then incubated with fresh WT or Δ*ltn1* extracts in the presence of cycloheximide, for 30 min before denaturing flag IP. The same amount of second extract was added to supernatant and pellet fractions. All reactions (lanes 1–6) were equalized for ~20% (wt/vol) sucrose concentration. The IPed material was analyzed by immunoblot against Ub or flag.

translation and ubiquitylation system has been developed and used to test the effect of mutations in mammalian listerin on ribosome-associated quality control (20). Here, we present an in vitro system enabling the study of *S. cerevisiae* Ltn1 function using *Neurospora crassa* extracts. In addition to exhibiting higher translation and ubiquitylation activities compared with *S. cerevisiae* extracts, this system offers the advantage that, unlike mammalian systems, *Neurospora* can also be easily genetically manipulated, thus serving as a source of extracts either cleanly lacking or overexpressing defined components. Using this system, we show that ribosome-stalled nonstop translation products (NSPs) become ubiquitylated in an Ltn1-dependent manner while still ribosome-associated. Importantly, we provide biochemical evidence that Ltn1's conserved NTD is required for binding to 60S subunits, along with evidence supporting the model that 60S association is required for Ltn1-mediated NSP ubiquitylation. Finally, we provide a structural basis for the observations reported here regarding Ltn1 NTD mutations by determining the crystal structure of the 45-kDa Ltn1 NTD from budding yeast at 2.4-Å resolution. Modeling the Ltn1 NTD into RQC structures revealed a highly conserved, positively charged surface that interacts with the phosphate backbone of the SRL, mutation of which disrupts Ltn1 function. Despite conservation of the Ltn1 NTD among eukaryotes, comparison of yeast and mammalian RQC structures revealed differences in the extreme N terminus that suggest that fungal and metazoan Ltn1 proteins use divergent mechanisms to interact with Rqc2.

Results

Newly Synthesized NSPs Are Ubiquitylated in *N. crassa* Extracts in an Ltn1-Dependent Manner. *Neurospora* extracts were used to study the fate of newly synthesized nonstop translation products (NSPs). We used templates for in vitro translation consisting of sequences encoding a flag tag and the first 53 residues of GFP, followed or not by four stop codons, and by a poly(A) tail of defined length (36 adenines). Thus, translation of the nonstop template resulted in as many as 12 lysines encoded by the poly(A) tail becoming fused to the C terminus of flag-GFP (fGFP-K12) (Fig. 1*A*).

The control reporter fGFP-s ("s" denoting the presence of stop codons) and fGFP-K12 were synthesized at comparable levels in the extracts (Fig. 1*B*). The anti-flag tag blot failed to reveal a slower migrating ladder or smear associated with fGFP-K12, which might be indicative of ubiquitylation. The inability to detect such an obvious ubiquitylation signature could have been due to inefficient NSP ubiquitylation, or to NSP deubiquitylation by ubiquitin proteases in the extract. We thus used a more sensitive and commonly used method to verify whether NSPs became ubiquitylated in *Neurospora* extracts. The flag-tagged translational products of fGFP-K12 and FGFP-s were immunoprecipitated (IPed) with flag antibody under denaturing conditions and analyzed by Western blot with anti-ubiquitin antibody. The results in Fig. 1*B* show that the NSP reporter fGFP-K12 was indeed ubiquitylated and that it was ubiquitylated to a greater extent than the reporter containing stop codons.

To test whether ubiquitylation of fGFP-K12 was Ltn1-dependent, translation was carried out in extracts prepared from an Ltn1-deficient isogenic strain (Δ*ltn1; N. crassa* Ltn1 is NCU06534). Although reporter proteins were synthesized normally in *N. crassa* extracts lacking Ltn1, ubiquitylation of NSPs was defective (Fig. 1*B*). Similar results were observed with two independently prepared batches of extracts. We note that, under these conditions, we have not observed a smear running immediately above the fGFP-K12 reporter band in either WT or Ltn1-deficient extracts, which might be attributed to Rqc2-mediated C-terminal extension with alanines and threonines ("CAT tails") (21). Likewise, we have not observed high molecular weight aggregates that could have been formed in a CAT tail-dependent manner (22, 23) (e.g., see Fig. 1*B*).

The inability of Δ*ltn1* extracts to mediate NSP ubiquitylation might have been due to the presence of a *trans*-acting inhibitor; however, arguing against this possibility, mixing Δ*ltn1* and WT extracts at a 1:1 ratio did not prevent fGFP-K12 ubiquitylation (Fig. 1*C*). Importantly, Δ*ltn1* extracts were verified to be fully competent for de novo ubiquitylation, as measured by the ability of exogenously supplied GST-tagged ubiquitin to be ligated to unknown proteins in the extract (Fig. 1*D*). Finally, to more decisively confirm that the inability of Δ*ltn1* extracts to promote ubiquitylation of fGFP-K12 was due to the absence of Ltn1, we tested whether addition of *Escherichia coli*-expressed, recombinant budding yeast (*S. cerevisiae*) Ltn1 to the reaction would suffice to restore fGFP-K12 ubiquitylation activity. The results in Fig. 1*E* show that full-length Ltn1 did in fact stimulate ubiquitylation of fGFP-K12 in Δ*ltn1* extracts; on the other hand, a mutated Ltn1 lacking the catalytic RING domain (Ltn1-ΔR) that is deficient in E3 activity but competent to bind to 60S subunits (2) failed to restore fGFP-K12 ubiquitylation under these conditions. Therefore, recapitulating the in vivo results with budding yeast, Ltn1 acts as the critical E3 mediating NSP ubiquitylation in *Neurospora* extracts.

Proteins encoded by normal, stop codon-containing mRNA, but harboring sufficiently long internal polybasic tracts, have also been characterized as Ltn1 substrates (11, 13). Thus, the ubiquitylation of proteins harboring polybasic tracts was also examined in the *Neurospora* system. Extracts were programmed with templates encoding fGFP appended with a C-terminal tract of 12 Lys or Arg (or Glu as negative control), followed by four stop codons ("s"). As predicted, and further demonstrating the specificity of this in vitro system, fGFP-K12-s and fGFP-R12-s—but not fGFP-E12-s—became ubiquitylated in an Ltn1-dependent manner (Fig. 1*F*).

Ltn1-Mediated NSP Ubiquitylation Occurs on Ribosomes. To provide further evidence that Ltn1-mediated NSP ubiquitylation begins on ribosomes, in one set of experiments, fGFP-K12 was translated in WT or Δ*ltn1* extracts and subjected to sucrose gradient sedimentation. Analysis of the fractions (Fig. 2*A*, *Lower*, "Input") indicated the greater presence of unmodified fGFP-K12 in ribosomal fractions in Δ*ltn1* compared with WT extracts. Unmodified fGFP-K12 in ribosomal fractions was also observed in Δ*ltn1* extracts supplemented with the recombinant, E3 ligase-deficient Ltn1-ΔR, but not with Ltn1 WT (Fig. 2*B*). Moreover, these results correlated with the observation that greater amounts of tRNA-linked fGFP-K12 were present in ribosome-containing pellets after sucrose cushion centrifugation of Δ*ltn1* compared with WT extracts (Fig. 2*C*).

Individual fractions of the gradient shown in Fig. 2*A*, *Lower* were also analyzed for fGFP-K12 ubiquitylation by carrying out denaturing flag IP, followed by anti-ubiquitin blot (Fig. 2*A*, *Upper*). The results revealed that ribosome-cofractionating fGFP-K12 (fractions 5–8) was ubiquitin-modified in WT but not the Δ*ltn1* extract (Fig. 2*A*, *Upper)* [this finding is in contrast to the total ubiquitin signal in the input fractions (Fig. 2*A*, *Lower*), which was unaffected by the absence of Ltn1]; this finding supports the model that Ltn1-mediated NSP ubiquitylation occurs on ribosomes.

Notably, the majority of the ubiquitylated fGFP-K12 signal was present in ribosome-free fractions at the top of the gradient (Fig. 2*A*, *Top Left*, fractions 1 and 2). Although this result is consistent with the model that ubiquitylation stimulates the release of stalled nascent chains from ribosomes (e.g., refs. 2, 11, 12, and 18), these results could not rule out the alternative possibility that much of fGFP-K12 became ubiquitylated subsequently to being released from ribosomes. To distinguish these possibilities, we developed a different assay. We first verified that fGFP-K12 synthesized in Δ*ltn1* extract could become ubiquitylated upon subsequent mixing with WT extract providing Ltn1 (in the presence of cycloheximide to prevent new translation) (Fig. 2*D*, lanes 1 and 2). Next, fGFP-K12 synthesized in the Δ*ltn1* extract was subjected to centrifugation through a sucrose cushion, and then the supernatant (containing ribosome-free fGFP-K12) and resuspended pellet (containing ribosome-bound fGFP-K12) were collected and incubated with WT extract for ubiquitylation to proceed. The results show that ribosome-associated fGFP-K12 was readily ubiquitylated upon subsequent mixing with WT extract (Fig. 2*D*, lane 5); in contrast, free (and more abundant) fGFP-K12 present in the supernatant was not ubiquitylated (Fig. 2*D*, lane 3). These results provide further evidence that Ltn1-mediated NSP ubiquitylation requires NSP presentation on ribosomes and that it takes place on ribosomes as well.

Ltn1 Requires an Intact N Terminus for NSP Ubiquitylation. We next began a structure–function analysis of Ltn1. In addition to the C-terminal RWD and RING domains, Ltn1's NTD is conserved from yeast to humans (Fig. S1 and ref. 2). The requirement of an intact NTD for Ltn1-mediated NSP ubiquitylation was therefore tested in the *Neurospora* system. For this purpose, we used flag-tagged WT yeast Ltn1 (amino acids 1–1562) and an NTD-deleted mutant (Ltn1-ΔN; amino acids 477–1562) that were both expressed and purified from *E. coli*. Previous structural characterization had revealed no obvious differences between Ltn1 WT and Ltn1-ΔN other than the absence of the deleted N-terminal region (7). Ltn1-ΔN was as competent as the WT protein in mediating ubiquitylation in the absence of added ribosomes or NSPs (Fig. 3*A*) (these reaction products presumably result from autoubiquitylation, based on observations with several other E3 ligases under similar reaction conditions, containing few pure components and no canonical substrate). As shown in Fig. 3*B* (and in Fig. 1*E*), addition of recombinant WT yeast Ltn1 to a Δ*ltn1* extract restored fGFP-K12 ubiquitylation, which required Ltn1's RING domain. In contrast, Ltn1-ΔN failed to restore fGFP-K12 ubiquitylation under these conditions (Fig. 3*B*), despite the fact that the Ltn1-ΔN mutant has an E3-active RING domain (Fig. 3*A*).

We extended these analyses by testing the effects of mutating an Ltn1 NTD highly conserved residue (Ltn1 T61A) (Fig. 3*C*). We selected Thr61 (in the yeast numbering), based on the rationale that

a hydrophilic residue would be more likely to be surface-exposed (an expectation confirmed by the NTD structure presented further below) and thus less prone to affect the domain's overall structure when mutated. Like the WT protein and the mutant lacking the entire NTD, Ltn1 T61A was competent for autoubiquitylation (Fig. 3*A*). Furthermore, like Ltn1-ΔN, Ltn1 T61A was less efficient in restoring fGFP-K12 ubiquitylation in a Δ*ltn1* extract (Fig. 3*B*). Thus, an intact NTD is required for Ltn1 function in NSP ubiquitylation.

Ltn1 NTD Mutations Interfere with 60S Binding. Ltn1 ubiquitylates ribosome-stalled NSPs in an NTD-dependent manner (Fig. 3 and ref. 24). Although predicted by the RQC structures, the NTD requirement for Ltn1 binding to the complex has not been experimentally tested. Because Ltn1 NTD mutants exhibited intact autoubiquitylation activity, we tested whether their failure to ubiquitylate NSPs was a consequence of defective 60S binding.

Flag-tagged WT or NTD mutant Ltn1 proteins were incubated with Δ*ltn1 Neurospora* extracts and subjected to sucrose gradient centrifugation. Fractions were collected and analyzed by anti-flag immunoblot (Fig. 4*A*). Ltn1-independent, flag cross-reacting bands, present in Fig. 4*A*, fractions 1–4, are marked with asterisks (see also Fig. S2). As expected, Ltn1 added to the Δ*ltn1* extract was predominantly found in the 60S fractions (Fig. 4*A* and, e.g., refs. 2 and 11–13). Importantly, compared with Ltn1 WT, both Ltn1 T61A and Ltn1-ΔN mutants exhibited decreased association with the 60S fraction (quantitation for Ltn1 WT and T61A presented in Fig. 4*B*).

Defective cofractionation of Ltn1 NTD mutants with 60S subunits was independently confirmed by assessing Ltn1's ability to co-IP with Rpl3 (Fig. 4*C*). Thus, these results suggest that Ltn1's conserved N terminus is important for RQC binding and, together with the results in Fig. 3 that NTD mutants do not ubiquitylate stalled NSPs, substantiate the model that NSP ubiquitylation is mediated by Ltn1 binding to stalled 60S subunits.

Structure of the Ltn1 N-Terminal Domain. Having found that an intact Ltn1 NTD was required for binding to 60S subunits and stalled nascent chain ubiquitylation, we set out to further characterize this function by determining the structure of the NTD to elucidate positions for its conserved residues, including Thr61, and how it interacts with the RQC complex. Limited proteolysis and N-terminal sequencing of full-length Ltn1 and an Ltn1 construct consisting of residues 1–440 enabled the identification of a stable domain that includes residues 13–424. Crystals of $Ltn1_{13–424}$ were obtained, and a structure was determined using single-wavelength anomalous dispersion (SAD) with selenomethionine-substituted (SeMet) protein (*SI Experimental Procedures*). SeMet $Ltn1_{13–424}$ crystallized in space group $P3_121$ and contained one molecule in the asymmetric unit. The structure included amino acid residues 14–419 and was refined at 2.5-Å resolution to an R_{work}/R_{free} of 0.20/0.24 and with good stereochemistry (Table 1). Native $Ltn1_{13–424}$ was solved by molecular replacement using SeMet Ltn1 coordinates as a search model in PHASER (25). Native $Ltn1_{13–424}$ crystallized in space group $P2_1$, contained two molecules in the asymmetric unit, and refined at 2.4-Å resolution to an R_{work}/R_{free} of 0.18/0.21 and with good stereochemistry (Table 1). Amino acids 14–420 were observed for both protomers in the asymmetric unit.

The Ltn1 NTD is predominantly composed of α-helices that are arranged into HEAT repeats (Fig. 5). HEAT repeats consist of two antiparallel α-helices that pack against each other in a repeating array. Overall, the Ltn1 NTD adopts a slightly curved topology with an outer and inner surface, an architecture frequently observed for other HEAT repeat-containing proteins (26). Residues 14–242 form a globular subdomain containing an N-terminal region that lacks a defined secondary structure, followed by four pairs of HEAT repeats (Fig. 5). The most N-terminal residues in the structure (residues 14–35) adopt a loop configuration that packs against helices a5, a7, a8, a11, and a12 through primarily hydrophobic interactions mediated by Leu18, Val23, Ile25, Leu27, and Tyr29. This globular subdomain is followed by an extended subdomain that includes four canonical HEAT repeat pairs. Although the primary sequence of the globular subdomain is conserved across evolution, the sequence of the extended HEAT repeats is only weakly conserved (7).

Budding yeast Ltn1 NTD adopts an overall fold similar to the partial poly-alanine model of human listerin NTD (Fig. S3) that was modeled based on electron density maps of the mammalian RQC EM structure (20). Although the primary amino acid sequence was not assigned in the structure of the human protein due to the relatively low resolution of the map in the NTD region, budding yeast Ltn1 NTD from residues 34–347 aligned well with its human counterpart, with an rmsd of 2.4 Å, enabling our tentative assignment of amino acid positions within the human

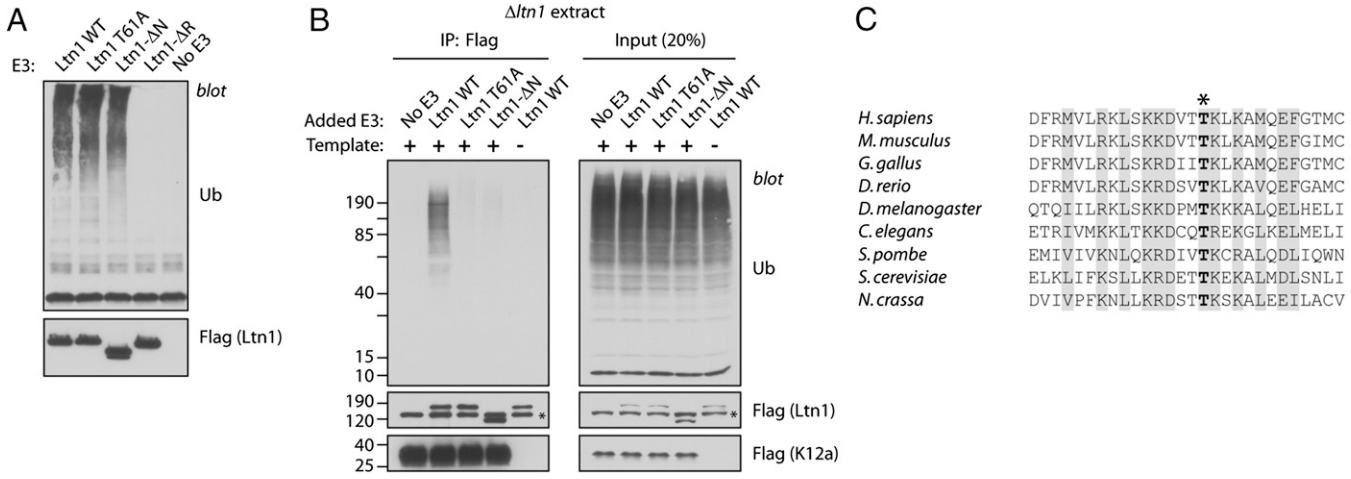

Fig. 3. Ltn1 requires an intact N terminus for NSP ubiquitylation. (*A*) The conserved Ltn1 N-terminal domain (NTD) is not required for autoubiquitylation activity. In vitro ubiquitylation assay containing *E. coli*-expressed E1, E2 (Ubc4), GST-Ub, and C-terminal flag-tagged yeast Ltn1. The Ltn1 proteins used were WT (amino acids 1–1562), NTD-deleted mutant (Ltn1-ΔN; amino acids 477–1562), T61A mutant, and RING domain-deleted mutant (Ltn1-ΔR; amino acids 1–1502). (*B*) An intact NTD is required for Ltn1 function in NSP ubiquitylation. fGFP-K12–encoding mRNA (500 ng; full-length GFP used) was translated in Δ*ltn1* extract [50 μL supplemented with 40 nM recombinant Ltn1 (WT or mutants, as in "A") for 30 min] and analyzed for ubiquitylation by denaturing flag IP as in Fig. 1*B*. The control reaction in lanes 5 lacked fGFP-K12 template mRNA. (*C*) Alignment showing evolutionary conservation of Thr61 (bold, asterisk) and neighboring residues (46–73 in yeast) in selected Ltn1 orthologs.

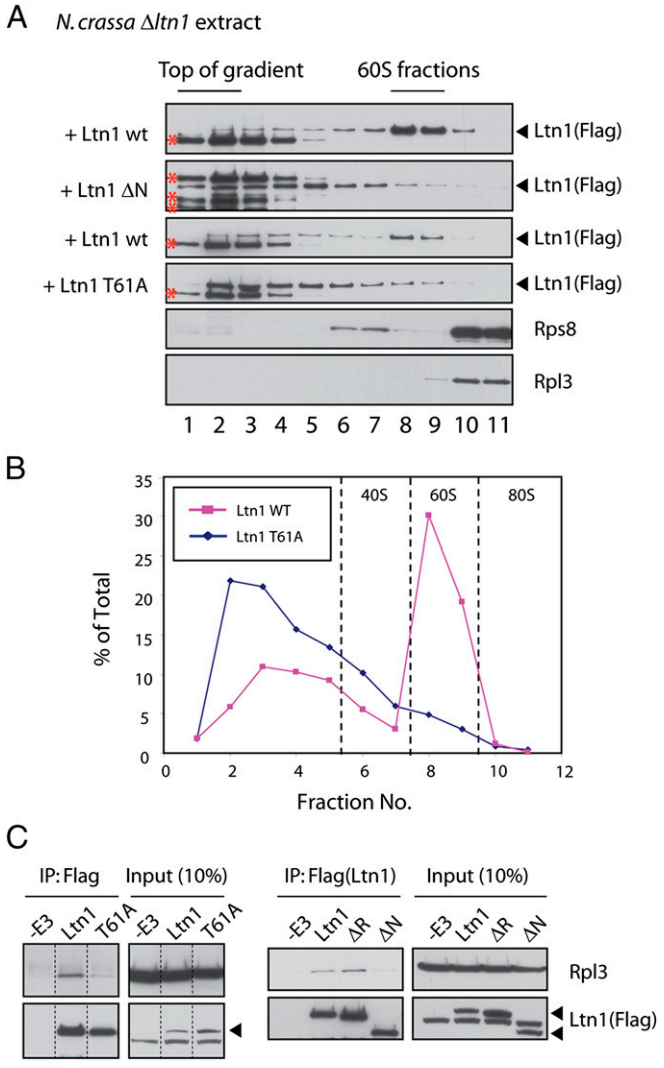

Fig. 4. Ltn1 NTD mutations interfere with ribosome binding. (*A*) An intact NTD domain is required for Ltn1 to cofractionate with 60S ribosomes as measured by sucrose gradient centrifugation. Flag-tagged Ltn1 WT or NTD mutants (40 nM) were incubated with 50 μL of Δ*ltn1* extracts for 15 min and subjected to centrifugation on 10–30% (wt/vol) sucrose gradient. Fractions were analyzed by immunoblot against flag, the 60S ribosomal protein Rpl3, or the 40S ribosomal protein Rps8. Ltn1-independent, flag cross-reacting bands present mostly in fractions 1–4 are marked with asterisks. (*B*) Graphic representation of results in the *Lower* panels of *A*. (*C*) An intact NTD domain is required for Ltn1 to co-IP with the 60S ribosomal protein Rpl3. Fifty microliters of Δ*ltn1* extract were incubated with flag-tagged Ltn1 WT or NTD mutants (40 nM) for 15 min. Ltn1 was IPed with antibody against flag and IP products analyzed by immunoblot against flag (Ltn1) or Rpl3. Dashed lines indicate that lanes were removed from the original image.

Ltn1 structure (Fig. S3). Human and yeast Ltn1 aligned best within the conserved globular domain whereas the extended HEAT repeats diverged somewhat. Despite the similarities between human and yeast Ltn1 NTD structures, fungal Ltn1 proteins differed in sequence and structure at their extreme N termini compared with higher eukaryotes (Fig. S3*B*). Human listerin has an additional 18 unique residues at its N terminus, and, in the human Ltn1 structure, residues 13–27 adopt a loop-α-helix structure that is not observed in the overall fold of yeast Ltn1 NTD (Fig. S3*A*). Conversely, although the loop made up of residues 14–35 in yeast Ltn1 seems part of the globular subdomain, this loop conformation is not observed in the human NTD structure.

Ltn1 Recognition of the 60S Component of the RQC. The NTD of human and yeast Ltn1 orthologs directly contact components of the RQC complex (19, 20, 24) and has been shown to be important for proper function of human Ltn1 with respect to stalled polypeptide ubiquitylation (20). The data in Fig. 4 show that the yeast Ltn1 NTD is important for association with ribosomes. To obtain higher resolution details on how Ltn1 binds to the RQC complex, we placed coordinates from the EM structure of the yeast 60S ribosomal subunit (PDB ID code 4V8T) and the Ltn1 NTD crystal structure generated here into EM maps of the yeast RQC by rigid body fitting. The Ltn1 NTD and the 60S ribosome fit well into the electron density and superposed with the orthologous proteins from the mammalian RQC structure (Fig. 6*A* and Fig. S4). As observed with the mammalian RQC (20), the Ltn1 NTD globular subdomain interacts with the SRL of the 23S rRNA (Fig. 6 *B* and *C*). The remaining NTD HEAT repeats extend away from the 60S

Table 1. Crystallographic data and refinement statistics

Dataset	Native	SeMet
Data collection*		
Source	APS 24IDC	APS 24IDC
Wavelength, Å	0.979	0.979
No. of crystals	1	1
Space group	$P2_1$	$P3_121$
Cell dimensions		
a,b,c, Å	88.51, 80.35, 97.33	58.1, 58.1, 347.1
α,β,γ, °	90, 116.58, 90	90, 90, 120
Resolution, Å	44.3–2.41 (2.49–2.41)	49.8–2.55 (2.64–2.55)
Completeness, %	98.0 (91.0)	99.0 (100.0)
Total reflections	150,619 (12,207)	221,836 (18,312)
Unique reflections	46,438 (4,285)	23,371 (2,261)
Wilson B-factor	47.3	58.8
Redundancy	3.2 (2.8)	9.5 (7.9)
R_{merge}, %	6.1 (41.6)	7.9 (56.8)
$CC_{1/2}$, %	99.8 (81.0)	99.9 (94.5)
CC*, %	100.0 (94.6)	100.0 (98.6)
$\langle I \rangle / \sigma(I)$	11.6 (2.3)	21.5 (3.5)
FOM (Phaser – 4 Se)		0.19
FOM (Resolve)		0.53
Refinement*		
Resolution, Å	44.3–2.41 (2.49–2.41)	49.8–2.55 (2.64–2.55)
No. of reflections (work/free)	44,530/1,880	22,174/1,152
R_{work}/R_{free}, %	17.6 (24.5)/21.2 (29.4)	20.2 (28.6)/24.3 (28.4)
No. of atoms	6,770	3,333
Protein	6,587	3,301
Ligand	14	1
Water	169	31
Average B-factors, $Å^2$	58.6	89.0
Protein	58.9	81.1
Ligand	58.4	75.7
Water	47.8	65.9
rmsd		
Bond lengths, Å	0.002	0.004
Bond angles, °	0.61	0.70
Molprobity†		
Favored, %	96.1 (778)	95.3 (385)
Allowed, %	100.0 (810)	100.0 (404)
Outliers, %	0.0 (0)	0.0 (0)
Clash score	100th percentile	100th percentile
Molprobity score	100th percentile	100th percentile
PDB code	5FG0	5FG1

*Statistics were calculated using Phenix (25); highest shell is indicated in parentheses; Friedel mates were averaged when calculating reflection statistics.
†Calculated with the program Molprobity (26).

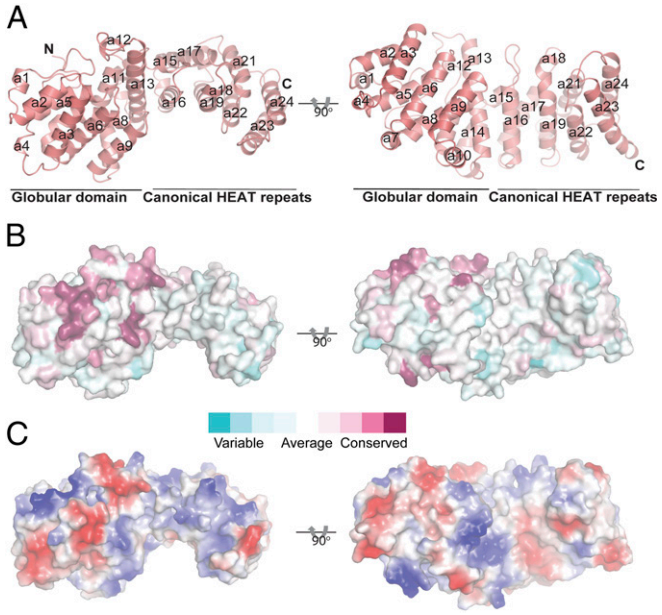

Fig. 5. Structure of the N-terminal domain of Ltn1. (*A*) The structure of the Ltn1 NTD depicted as a schematic model in two orientations. Helices are labeled from a1 to a24, N and C termini are labeled N and C, respectively. The N-terminal globular domain and C-terminal canonical HEAT repeat regions are indicated. (*B*) Surface representation of Ltn1 with the sequence conservation mapped onto the surface. (*C*) Surface representation of Ltn1 with the electrostatic potential mapped onto the surface, with blue and red indicating positive and negative potential, respectively.

ribosomal surface and terminate at the hinge point between the NTD and the elongated middle domain of Ltn1 (Fig. 6*A*).

Alignment of the primary sequence of Ltn1 orthologs reveals at least two main regions of high conservation on the Ltn1 surface between residues 49–64 (helices a2–a3) and 202–211 (helix a13) (Fig. 5*B* and Fig. S3*B*). In the model, conserved residues from Glu202 to Val211 are not involved in direct interactions with the 60S subunit whereas the other conserved region that includes residues Leu49 to Lys64 forms an α-helix-loop-α-helix element that directly contacts the SRL (Fig. 6*B*). The surface formed by the latter residues includes a positively charged patch in addition to other residues that could provide hydrogen bond donor/acceptor pairs and that are in suitable positions to make contacts with the phosphate backbone moieties of SRL nucleotides 3022–3028 (Fig. 6 *B* and *C*). The ε-amino group of Ltn1 Lys52 is within hydrogen-bonding distance to the phosphate backbone of A3024. Lys56 is also proximal to this position although it could also contact the phosphate backbones of U3023 and G3028. The Arg57 guanidinium group is buttressed by Tyr198 and is proximal to the G3028 backbone phosphate whereas Asp58 is proximal to the G3028 ribose. Supporting the functional analysis described above, we observed that the hydroxyl groups of Thr60 and Thr61 and the Lys64 side chain are proximal to the backbone phosphate of G3022 whereas Leu49 is within van der Waals (VDW) distance of His96 of the RPL8 ribosomal subunit. These residues are highly conserved from yeast to mammals, indicating that yeast and mammalian Ltn1 use a similar mechanism to directly engage the 60S ribosome.

To probe the importance of the aforementioned contacts in the NTD, we generated structure-guided NTD mutations within the context of recombinant, full-length Ltn1 harboring a Flag tag at the C terminus and examined their effect both on ribosome binding and on ubiquitylation of a stalled nascent chain reporter substrate using the in vitro *N. crassa* system as described in *Newly Synthesized NSPs Are Ubiquitylated in N. crassa Extracts in an Ltn1-Dependent Manner*.

The relative efficiency of ribosome binding by Ltn1 mutants was evaluated using limiting amounts of recombinant Ltn1 proteins mixed with Δ*ltn1* extracts and centrifuged over a sucrose cushion. The results in Fig. 7*A* show that, in this assay, the R57A and T61A mutants exhibited decreased binding to ribosomes, as revealed by the presence of a higher fraction of those proteins in the postcentrifugation supernatant compared with WT Ltn1. The effect of mutating Arg57 was more modest than mutating Thr61,

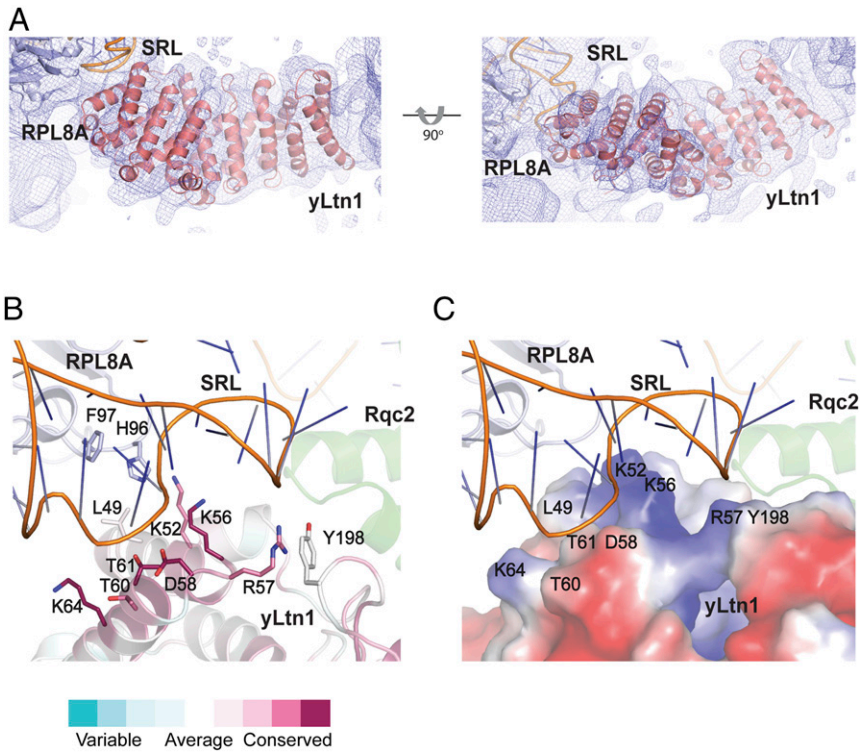

Fig. 6. Model for interactions between the Ltn1 NTD and 60S component of the RQC. (*A*) Schematic representation of the yeast RQC structure depicting the region where yeast Ltn1 (salmon) contacts the 60S ribosome. The sarcin-ricin loop (SRL) is colored orange, and Rpl8A is colored light blue. The EM map of the yeast RQC (EMD-6170) contoured to 1.5σ is displayed in blue showing the fit of the yeast 60S coordinates (PDB ID code 4V8T) and yeast Ltn1 NTD into the maps. The same model is displayed in the *Right* panel oriented 90° from the view shown in the *Left* panel. (*B*) Close-up of the interface of the SRL (orange) and Rpl8A (blue) with Ltn1. Ltn1 is shown as a diagram colored from teal to purple by the degree of sequence conservation (low to high). Ltn1 residues that contact the SRL and Rpl8 are shown as sticks, and the position of Rqc2 is shown as a diagram in green. (*C*) Same as in *B* but with the electrostatic potential mapped onto the surface of Ltn1.

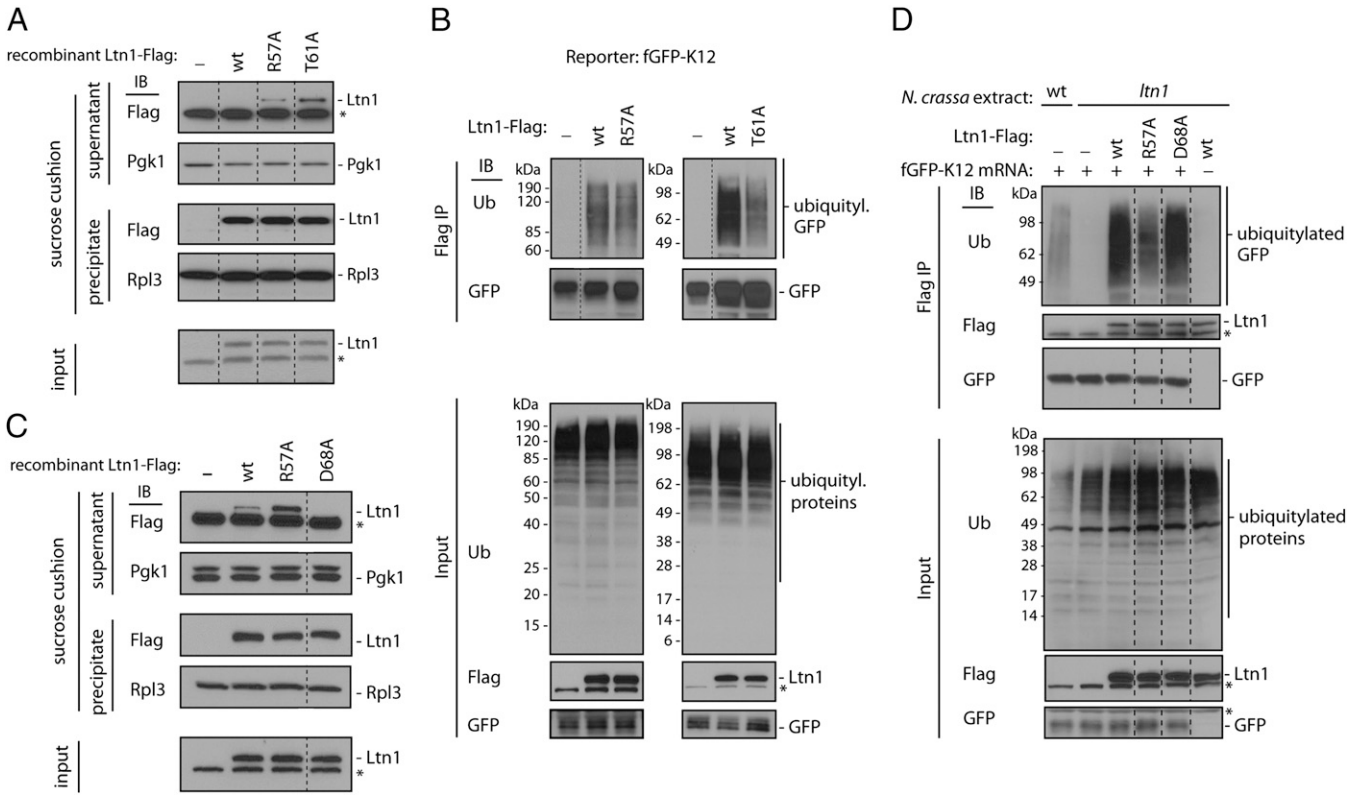

Fig. 7. Effect of mutations in Ltn1's SRL-binding surface on ribosome binding and nascent chain ubiquitylation. Dashed lines indicate that lanes were removed from the original image. (*A*) Mutations in Ltn1's SRL-binding surface affect ribosome binding as measured by sucrose gradient centrifugation. Flag-tagged Ltn1 WT or NTD mutants (R57A or T61A) were incubated with Δ*ltn1 Neurospora* extract and subjected to centrifugation on sucrose cushion, as described in *SI Experimental Procedures*. Input, supernatant, and pellet were analyzed by immunoblot against Flag (Ltn1), the 60S ribosomal protein Rpl3, or the cytosolic protein Pgk1. Ltn1-independent, anti-Flag antibody cross-reacting bands are marked with asterisks. (*B*) Mutations in Ltn1's SRL-binding surface affect stalled nascent chain ubiquitylation. Stalling reporter-encoding mRNA was translated in Δ*ltn1* extract supplemented or not with recombinant Ltn1 (WT, R57A mutant, or T61A mutant) and analyzed for ubiquitylation by denaturing IP (see also Fig. S5). Immunoblots were against Flag (Ltn1), Ubiquitin (Ub), and GFP (stalling reporter). (*C*) As in *A*, except that Ltn1 R57A and D68A mutants were analyzed. (*D*) As in *B*, except that Ltn1 R57A and D68A mutants were analyzed, the "no template mRNA" control is shown, and the WT extract was also used as positive control.

perhaps due to the presence of several other basic residues in this SRL-interacting patch.

We next investigated the extent to which the effect of Ltn1 mutations on ribosome binding correlated with defects in ubiquitylation of ribosome-stalled nascent chains. For this purpose, Δ*ltn1 Neurospora* extracts were mixed with Ltn1 WT or mutant proteins and programmed to translate the fGFP-K12 mRNA template (nonstop reporter). As in the experiments described in Figs. 1 and 2, in WT extract, but not Δ*ltn1* extract, nonstop reporter protein was ubiquitylated (see also Fig. S5, lanes 1 and 2). Reporter ubiquitylation could be restored in the Δ*ltn1* extract by addition of recombinant WT yeast Ltn1, but not by a Ltn1 mutant lacking the RING domain (Ltn1 ΔRING) (Fig. S5, lanes 3 and 4). Ubiquitylation defects were apparent for the Ltn1 R57A and, to a greater extent, Ltn1 T61A mutants (Fig. 7*B*), consistent with the importance of these conserved residues for mediating direct interactions with the 60S subunit (an additional mutation, K64A, yielded more modest and variable defects in this assay). We also tested the effect of mutating Asp68, whose negative charge is conserved among Ltn1 orthologs. Surprisingly, the Ltn1 D68A mutant seemed to exhibit improved binding to ribosomes compared with WT Ltn1 and was fully competent for reporter ubiquitylation (Fig. 7 *C* and *D*, respectively). One possibility to explain this observation is that the negative charge helps modulate Ltn1-60S binding toward an optimal, rather than maximal, extent by neutralizing the positive charge in the neighboring basic patch. For comparison, substitution of additional selected conserved residues that are exposed elsewhere on the NTD surface (Ltn1 K130A, E202A, and E205A mutants) revealed no obvious consequence in these assays (Fig. S5, lanes 5–7).

Ltn1 Interaction with Rqc2. Rqc2 increases association of Ltn1 to the RQC complex and enhances ubiquitylation of stalled nascent chains (11, 12). In the RQC, Ltn1 and Rqc2 interact with each other near the SRL in a position such that surfaces important for 40S ribosomal subunit association become sterically occluded (19, 21). We placed a model of *S. cerevisiae* Rqc2 [obtained using the coordinates of human Rqc2 (NEMF)] into the yeast RQC maps using rigid body fitting. *S. cerevisiae* Rqc2 adopts a position similar to that observed for human Rqc2 in the mammalian RQC structure (Fig. 8*A* and Fig. S4*B*). Based on the cryo-EM structures, Rqc2 consists of an N-terminal NFACT-N domain that is believed to recruit Ala- or Thr-tRNA to the A site for CAT tail synthesis, and an additional density (that may include NFACT-R and perhaps also NFACT-C domains) that contacts the stalled P site tRNA (20, 21). Coiled-coils extend from these domains and connect them to a globular middle domain (M-domain) that makes multiple interactions with Ltn1, the SRL, and the P stalk of the 60S ribosome (20).

Although it is clear that the ability of Ltn1 to interact with the 60S ribosome and Rqc2 components of the RQC is shared among eukaryotes, the Ltn1–Rqc2 interaction surface does not seem to be fully conserved. *S. cerevisiae* Ltn1 residues 30–36, which form an interaction interface for Rqc2, are strongly conserved in fungi and less conserved in higher eukaryotes (Fig. 8*D* and Fig. S3*B*). Furthermore, there seems to be no structural

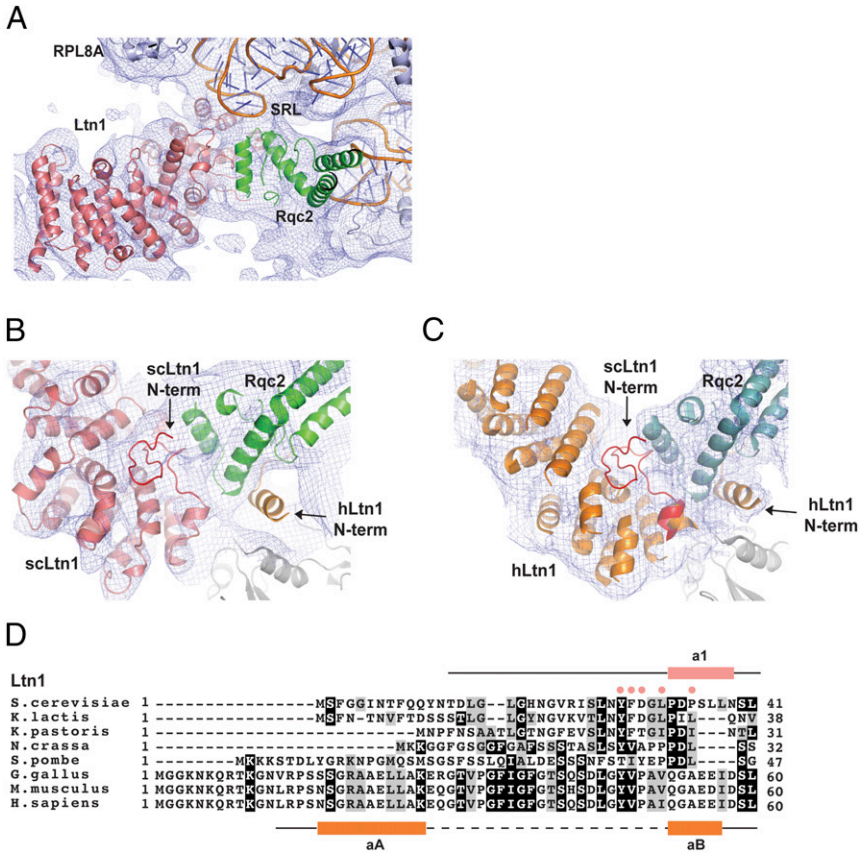

Fig. 8. Model for interactions between Ltn1 and Rqc2. (*A*) Schematic representation of the interaction of yeast Ltn1 (salmon) with a model of yeast Rqc2 (green) and the SRL. The EM map of the yeast RQC (EMD-6170) contoured to 1.5σ is displayed in blue showing the fit of the proteins in the maps. (*B* and *C*) Comparison of the Ltn1-Rqc2 interface and the Ltn1 N termini in yeast versus mammals. (*B*) Schematic representation of yeast Ltn1 (salmon) and Rqc2 (green). The EM map of the yeast RQC contoured to 1.5σ is displayed in blue, and Ltn1 residues 14–35 are colored red, highlighting the presence of electron density for this region. The position of the extreme N-terminal helix (orange) of the human Ltn1 NTD based on an alignment with the yeast RQC is indicated by an arrow demonstrating the lack of electron density in this region of the map. (*C*) Schematic representation of the human Ltn1 (orange) and Rqc2 (teal) interface (PDB ID code 3J92) with the EM map from the mammalian RQC (EMD-2832) contoured at 1.5σ. The position of the extreme N terminus from yeast Ltn1 is shown in red, and the human Ltn1 extreme N terminus is indicated by an arrow. (*D*) Secondary structure-based sequence alignment of the N-terminal residues from yeast and metazoans. Conserved residues are highlighted in black (highly conserved) and gray (moderately conserved). The secondary structure of yeast Ltn1 is shown above the sequence alignment whereas that of the human structure is shown below. Ltn1 residues in the interface with Rqc2 in yeast are indicated by pink dots above the residues.

equivalent for this interaction when RQC complexes are compared. Electron density is present for the N-terminal yeast Ltn1 residues in the yeast RQC complex (Fig. 8*B*), but no electron density is evident in this region in the human RQC complex (Fig. 8*C*). Perhaps in lieu of this interface, metazoan Ltn1 residues 13–27 adopt an α-helix conformation that makes contacts with both Rqc2 and ribosomal subunit eL40, on the opposite surface of Rqc2 from where Ltn1 contacts Rqc2 in the yeast complex (Fig. 8*C*). This Ltn1 helix has been shown to be important for function in mammals but seems to be absent in yeast because there is neither sequence conservation nor electron density in the same position in the yeast RQC EM maps (Fig. 8*B*). Therefore, metazoan listerin seems to have evolved a unique manner to interact with its Rqc2 ortholog.

Discussion

Here, we present genetically modified *Neurospora* extracts as a system to study RQC and use this system to provide biochemical evidence that Ltn1's conserved NTD is required for binding to 60S subunits. Importantly, we determined the 2.4-Å X-ray crystal structure of the Ltn1 NTD; by modeling the NTD structure onto available lower resolution RQC complex structures, we now provide more detailed information on how Ltn1 interacts both with the 60S subunit and with its RQC complex cofactor, Rqc2. Finally, we present evidence supporting the model that 60S association is required for Ltn1-mediated ubiquitylation of stalled nascent chains, which we also show as taking place on ribosomes.

A New System to Study Ribosome-Associated Quality Control. We describe a system enabling elucidation of mechanisms underlying the fungal Ltn1 pathway using translation- and ubiquitylation-competent *Neurospora* cell-free extracts. Importantly, *Neurospora* can be manipulated genetically with relative ease, allowing one to generate custom extracts that are cleanly altered for specific factors of interest. Indeed, using WT and Δ*ltn1* extracts, we were able to reconstitute essential features of the Ltn1 pathway elucidated in previous studies and to biochemically substantiate aspects of the proposed model of Ltn1 function. We first showed that NSP ubiquitylation was defective in Δ*ltn1* extracts. Adding power to the analyses, it was possible to rescue the defect by adding to the reaction recombinant yeast Ltn1 purified from *E. coli*. Finally, we have also been able to use this system to provide direct physical evidence for an important role for Ltn1's conserved NTD in 60S binding and substrate targeting.

A Structural Basis for Ltn1 NTD Interactions with the Ribosome. Cryo-EM structures of Ltn1/listerin in complex with other RQC subunits and the stalled 60S show that Ltn1 is an extended molecule spanning the distance from the vicinity of the intersubunit surface to the opening of the ribosomal exit tunnel (19–21), as we had previously proposed (7). Furthermore, those structures show that Ltn1's conserved NTD and CTD domains bind to other components of the complex, with the NTD binding directly both to the 60S subunit near the SRL, as well as to the Rqc2/NEMF subunit.

Accordingly, in the work presented here, we observed a requirement for the Ltn1 NTD in 60S association. Furthermore, mutation of the conserved Ltn1 Thr61 residue was sufficient to cause defects in both complex binding and NSP ubiquitylation. At the resolution of the RQC complex cryo-EM structures that have been solved, it had not been possible to assign specific function to the conserved NTD residues, so the exact role of the Ltn1 Thr61 residue was not clear. The crystal structure reported here, analyzed in conjunction with the cryo-EM structures of RQC complexes from human and yeast, sheds additional light on NTD function. Among other findings, it shows that the Thr61 side chain hydroxyl group is indeed proximal to the SRL of the 60S subunit.

The 2.4-Å X-ray crystal structure of the yeast Ltn1 NTD has revealed that Thr61 belongs to a conserved surface. Although interactions with the SRL of the 60S subunit provide a plausible

explanation for the conservation of such a surface, the structure revealed additional conserved surfaces on the Ltn1 NTD, which warrant further investigation because they suggest alternative strategies that Ltn1 may use for stable association with the RQC; alternatively, these surfaces may be conserved for other functions.

Comparison of the yeast Ltn1 NTD with the analogous domain of human listerin showed similarity throughout most of the structure although it is clear that the extreme N-terminal segments differ in primary amino acid composition (human listerin includes an additional ∼15 aa), structure, and function. Although human listerin includes an amphipathic helix that tucks under human Rqc2, this element is not apparent in the EM density of the yeast complex, and yeast Ltn1 seems to have a unique N-terminal segment that packs into the Ltn1 globular domain near the interface with yeast Rqc2. Although our structure of *S. cerevisiae* Ltn1 does not include the N-terminal 12 amino acids, sequence comparison with the human protein does not reveal significant similarity in this region, consistent with the model that yeast Ltn1 does not use an N-terminal helix for interaction with Rqc2. This latter point is also supported by the apparent lack of electron density for this segment in a higher resolution EM structure of yeast Ltn1 in complex with the RQC (21).

In contrast to the results presented here with yeast Ltn1, neither a triple mutation of conserved human listerin NTD residues nor deletion of most of the NTD affected NSP ubiquitylation in the mammalian system; it was only when NTD and CTD mutations were combined that a defect in NSP ubiquitylation was observed (20). It remains to be determined whether the stronger dependency on the Ltn1 NTD that we observed results from innate differences between the fungal and mammalian systems, such as the structural differences described in the preceding paragraph, or whether this dependency is due to differences in the sensitivities of the assay procedures.

Ribosome-Associated Ubiquitylation. We provide here two lines of evidence supporting the model that stalled nascent chains are presented to Ltn1 and become ubiquitylated while still associated with the 60S subunit. First, we demonstrated a requirement for NSP presentation on ribosomes in order for Ltn1-mediated ubiquitylation to take place because Ltn1 was unable to ubiquitylate NSPs when mixed subsequently with NSPs that had been released from ribosomes. Second, we generated Ltn1 NTD mutants that are defective in 60S binding and showed that these NTD mutations impaired NSP ubiquitylation. Ltn1's ability to target its protein quality control substrates while the latter are still 60S-associated ensures that aberrant proteins are marked for degradation before being released in the cytosol, where they might escape proteolysis and engage in detrimental interactions. Furthermore, by using 60S subunits as adapters, Ltn1 is able to target a large variety of nascent polypeptides that can become stalled during translation. These findings contribute toward our understanding of how E3s that function in protein quality control are able to recognize heterogeneous substrates—an important, yet unresolved, problem.

Experimental Procedures

In vitro translation with *Neurospora* extracts, preparation of recombinant yeast Ltn1, Ltn1-ribosome binding assays, denaturing IP, analysis of peptidyl-tRNA conjugates, an in vitro ubiquitylation assay with recombinant proteins, and protein crystallization are described in *SI Experimental Procedures*.

ACKNOWLEDGMENTS. We thank G. Dieci and J. Warner for reagents and the Fungal Genetics Stock Center for providing *Neurospora* strains. Work in the C.A.P.J. laboratory is supported by R01 Grant NS075719 from the National Institute of Neurological Disorders and Stroke (NINDS) of the NIH and R01 Grant CA152103 from the National Cancer Institute (NCI) of the NIH. Work in the M.S.S. laboratory is supported by P01 Grant GM068087. Work in the C.D.L. laboratory is supported by NIH Grant R01 GM061906 and NIH/NCI Cancer Center Support Grant P30 CA008748. X-ray crystallographic work is based upon research conducted at the Northeastern Collaborative Access Team beamlines, which are funded by the National Institute of General Medical Sciences from the National Institutes of Health (Grant P41 GM103403). The Pilatus 6M detector on the 24-ID-C beamline is funded by NIH-ORIP HEI Grant S10 RR029205. This research used resources of the Advanced Photon Source, a US Department of Energy (DOE) Office of Science User Facility operated for the DOE Office of Science by Argonne National Laboratory under Contract DE-AC02-06CH11357. C.D.L. is an investigator of the Howard Hughes Medical Institute. This is manuscript 28002 from The Scripps Research Institute. The content is solely the responsibility of the authors and does not necessarily represent the official views of the National Institutes of Health.

1. Chu J, et al. (2009) A mouse forward genetics screen identifies LISTERIN as an E3 ubiquitin ligase involved in neurodegeneration. *Proc Natl Acad Sci USA* 106(7):2097–2103.
2. Bengtson MH, Joazeiro CA (2010) Role of a ribosome-associated E3 ubiquitin ligase in protein quality control. *Nature* 467(7314):470–473.
3. Wang F, Canadeo LA, Huibregtse JM (2015) Ubiquitination of newly synthesized proteins at the ribosome. *Biochimie* 114(Jul):127–133.
4. Wolff S, Weissman JS, Dillin A (2014) Differential scales of protein quality control. *Cell* 157(1):52–64.
5. Lykke-Andersen J, Bennett EJ (2014) Protecting the proteome: Eukaryotic cotranslational quality control pathways. *J Cell Biol* 204(4):467–476.
6. Brandman O, Hegde RS (2016) Ribosome-associated protein quality control. *Nat Struct Mol Biol* 23(1):7–15.
7. Lyumkis D, et al. (2013) Single-particle EM reveals extensive conformational variability of the Ltn1 E3 ligase. *Proc Natl Acad Sci USA* 110(5):1702–1707.
8. Lu J, Deutsch C (2008) Electrostatics in the ribosomal tunnel modulate chain elongation rates. *J Mol Biol* 384(1):73–86.
9. Charneski CA, Hurst LD (2013) Positively charged residues are the major determinants of ribosomal velocity. *PLoS Biol* 11(3):e1001508.
10. Edenberg ER, Downey M, Toczyski D (2014) Polymerase stalling during replication, transcription and translation. *Curr Biol* 24(10):R445–R452.
11. Brandman O, et al. (2012) A ribosome-bound quality control complex triggers degradation of nascent peptides and signals translation stress. *Cell* 151(5):1042–1054.
12. Defenouillère Q, et al. (2013) Cdc48-associated complex bound to 60S particles is required for the clearance of aberrant translation products. *Proc Natl Acad Sci USA* 110(13):5046–5051.
13. Shao S, von der Malsburg K, Hegde RS (2013) Listerin-dependent nascent protein ubiquitination relies on ribosome subunit dissociation. *Mol Cell* 50(5):637–648.
14. Letzring DP, Wolf AS, Brule CE, Grayhack EJ (2013) Translation of CGA codon repeats in yeast involves quality control components and ribosomal protein L1. *RNA* 19(9):1208–1217.
15. Becker T, et al. (2011) Structure of the no-go mRNA decay complex Dom34-Hbs1 bound to a stalled 80S ribosome. *Nat Struct Mol Biol* 18(6):715–720.
16. Shoemaker CJ, Eyler DE, Green R (2010) Dom34:Hbs1 promotes subunit dissociation and peptidyl-tRNA drop-off to initiate no-go decay. *Science* 330(6002):369–372.
17. Pisareva VP, Skabkin MA, Hellen CU, Pestova TV, Pisarev AV (2011) Dissociation by Pelota, Hbs1 and ABCE1 of mammalian vacant 80S ribosomes and stalled elongation complexes. *EMBO J* 30(9):1804–1817.
18. Verma R, Oania RS, Kolawa NJ, Deshaies RJ (2013) Cdc48/p97 promotes degradation of aberrant nascent polypeptides bound to the ribosome. *eLife* 2:e00308.
19. Lyumkis D, et al. (2014) Structural basis for translational surveillance by the large ribosomal subunit-associated protein quality control complex. *Proc Natl Acad Sci USA* 111(45):15981–15986.
20. Shao S, Brown A, Santhanam B, Hegde RS (2015) Structure and assembly pathway of the ribosome quality control complex. *Mol Cell* 57(3):433–444.
21. Shen PS, et al. (2015) Protein synthesis. Rqc2p and 60S ribosomal subunits mediate mRNA-independent elongation of nascent chains. *Science* 347(6217):75–78.
22. Yonashiro R, et al. (2016) The Rqc2/Tae2 subunit of the ribosome-associated quality control (RQC) complex marks ribosome-stalled nascent polypeptide chains for aggregation. *eLife* 5:e11794.
23. Choe YJ, et al. (2016) Failure of RQC machinery causes protein aggregation and proteotoxic stress. *Nature* 531(7593):191–195.
24. Shao S, Hegde RS (2014) Reconstitution of a minimal ribosome-associated ubiquitination pathway with purified factors. *Mol Cell* 55(6):880–890.
25. McCoy AJ, et al. (2007) Phaser crystallographic software. *J Appl Cryst* 40(Pt 4):658–674.
26. Andrade MA, Perez-Iratxeta C, Ponting CP (2001) Protein repeats: Structures, functions, and evolution. *J Struct Biol* 134(2-3):117–131.
27. Dieci G, Bottarelli L, Ottonello S (2005) A general procedure for the production of antibody reagents against eukaryotic ribosomal proteins. *Protein Pept Lett* 12(6):555–560.
28. Wu C, Amrani N, Jacobson A, Sachs MS (2007) The use of fungal in vitro systems for studying translational regulation. *Methods Enzymol* 429:203–225.
29. Mossessova E, Lima CD (2000) Ulp1-SUMO crystal structure and genetic analysis reveal conserved interactions and a regulatory element essential for cell growth in yeast. *Mol Cell* 5(5):865–876.
30. Hendrickson WA, Horton JR, LeMaster DM (1990) Selenomethionyl proteins produced for analysis by multiwavelength anomalous diffraction (MAD): A vehicle for direct determination of three-dimensional structure. *EMBO J* 9(5):1665–1672.
31. Otwinowski Z, Minor W (1997) Processing of X-ray diffraction data collected in oscillation mode. *Methods Enzymol* 276(Pt A):307–326.
32. Sheldrick GM (2008) A short history of SHELX. *Acta Crystallogr A* 64(Pt 1):112–122.
33. Emsley P, Cowtan K (2004) Coot: Model-building tools for molecular graphics. *Acta Crystallogr D Biol Crystallogr* 60(Pt 12, Pt 1):2126–2132.